Unraveling the auxin mechanism in 2,4-D induced somatic embryogenesis in Arabidopsis thaliana

Philipsen, C.

Chapter 4

Somatic embryogenesis initiation in *Arabidopsis* requires *SOLITARY ROOT/IAA14*-regulated dynamic auxin responses similar to lateral root initiation

Cheryl Philipsen[1,2],
Vera Veltkamp[1,3],
Tanja van den Nadort[1,4],
Remko Offringa[1]

[1] *Molecular and Developmental Genetics, Institute of Biology Leiden, Leiden University, Sylviusweg 72, 2333BE, Leiden, the Netherlands*
[2] *Current affiliation: Dümmen Orange, P.O. Box 26, 2678ZG, de Lier, the Netherlands*
[3] *Current affiliation: Plant Research International, P.O. Box 7, 1600AA Wageningen, the Netherlands*
[4] *Current affiliation: Leiden University Medical Centre, P.O. Box 9600, 2300 RC Leiden, the Netherlands*

Abstract

Somatic embryogenesis (SE), a process where embryos are induced on somatic plant tissues, is used for crop micropropagation to obtain genetically identical and uniform plants. SE is commonly induced by incubating explant tissues on high concentrations of the synthetic auxin analog 2,4-dichlorophenoxyacetic acid (2,4-D). Although previous research in *Arabidopsis* has revealed several genetic candidates involved in SE, the molecular mechanism by which 2,4-D induces SE is still largely unknown. Here we used a combination of chemical biology, mutants and promoter reporter lines to map the auxin response components involved in 2,4-D-induced SE on *Arabidopsis* immature zygotic embryos (IZEs). We employed the auxin antagonist auxinole, blocking the formation of TRANSPORT INHIBITOR RESISTANT1/AUXIN SIGNALING F-BOX (TIR1/AFB) co-receptor complex, and found that this co-receptor complex was required for SE initiation. Furthermore, we found that the activating *AUXIN RESPONSE FACTOR* (*ARF*) sister pairs *ARF7/19* and *ARF6/8* were both required for efficient SE initiation as well. Interestingly, SE was almost completely blocked in the semi-dominant *solitary root-1* (*slr-1*) mutant, indicating that 2,4-D-induced SE and lateral root initiation in *Arabidopsis* share the same auxin response module. The auxin response mutants that were blocked in SE also showed a reduced 2,4-D-induced root callus development, suggesting that this phenotype could be used to pre-select mutants affected in SE. Based on our results we propose a model in which *SLR/IAA14*–regulated dynamic auxin responses are required for both lateral root and embryonic founder cell specification and the subsequent cell divisions starting respectively lateral root and somatic embryo development.

Introduction

Somatic embryogenesis (SE) is a fascinating process in plants by which embryo development is induced on differentiated somatic tissues. In *Arabidopsis*, SE can be efficiently induced on immature zygotic embryos (IZEs) by culturing these IZEs on solid medium containing high concentrations of 2,4-dichlorophenoxyacetic acid (2,4-D), a synthetic analogue of the plant hormone auxin (Gaj, 2011). Subsequently, two SE programs can be observed: 1) direct SE (DSE) referring to somatic embryos formed directly from the epidermal cell layer of late IZEs, and 2) indirect SE (ISE) where somatic embryos are formed from embryonic callus that originates from the sub-epidermal layers of young IZEs (Kurczyńska et al., 2007; Raghavan, 2004). Similar to SE, plant regeneration via organogenesis can also occur directly from somatic cells or indirectly via a callus phase. Callus can be produced from a single differentiated cell and many of the derived callus cells are totipotent, being able to regenerate the whole plant body (Ikeuchi et al., 2013). Callus development during plant regeneration can be divided into three phases, which may also occur during SE. Firstly, in the dedifferentiation phase, somatic cells adopt a stem cell state in response to exogenously applied hormones. In the second phase, the callus cells are reprogrammed and determined to form a specific organ depending on the hormone balance in the medium. Several callus types exist that are classified as rooty, shooty, or embryonic callus, depending on the organs they regenerate, or as friable callus that does not regenerate organs. The third or morphogenesis phase of the regeneration process involves the actual formation of the new organs and occurs independent of exogenously applied hormones (Su and Zhang, 2014). Evidence has emerged that during the dedifferentiation phase, somatic cells are not completely dedifferentiated to an omnipotent stem cell state, but rather resemble the stem cells in the root pericycle that give rise to lateral root formation (Atta et al., 2008; Sugimoto et al., 2010; Ikeuchi et al., 2013). Cell dedifferentiation and cell fate specification involve the molecular regulation and action of the natural auxin indole-3-acetic acid (IAA).

Auxin is perceived in the nucleus of plant cells by the TRANSPORT INHIBITOR RESISTANT1/AUXIN SIGNALING F-BOX (TIR1/AFB) F-box proteins and the AUXIN/INDOLEACETIC ACID (AUX/IAA) auxin co-receptors. The *Arabidopsis* genome encodes 6 TIR1/AFB proteins, which together with one of the 29 AUX/IAA proteins from a hydrophobic binding pocket for auxin. TIR1/AFBs interact with other proteins (ASK1, CUL1, RBX) to form the $SCF^{TIR1/AFB}$ E3 ubiquitin protein ligase complex. In the presence of auxin, this complex recruits the Aux/IAA co-receptors and labels these repressor proteins by ubiquitination for degradation by the

26S proteasome (Maraschin et al., 2009; Dharmasiri et al., 2005a, 2005b; Parry et al., 2009). Most Aux/IAAs consist of three conserved domains. The N-terminal domain I (DI) is required for transcriptional repression and recruits co-repressor proteins like TOPLESS (TPL) and the middle domain II (DII) is responsible for protein stability and interacts directly with auxin and the TIR1/AFB auxin co-receptors (Wang and Estelle, 2014). Finally, through their conserved C terminal domain Aux/IAAs interact with Auxin Response Factors (ARFs) that bind to the auxin response elements (AuxREs) in the promoters of auxin responsive genes (Weijers and Wagner, 2016). Recently, evidence has emerged that both Aux/IAAs and ARFs form a type I/II Phox and Bem1p (PB1) protein-protein interaction domain in their C-terminus that is required for this interaction (Korasick et al., 2014).

The auxin-dependent Aux/IAA degradation releases repression of ARFs and allows transcriptional activation of auxin responsive genes. Each TIR1/AFB receptor has different binding affinities for specific Aux/IAA proteins (Calderón Villalobos et al., 2012; Parry et al., 2009). Furthermore, each TIR1/AFB – Aux/IAA co-receptor pair has a different binding affinity for the different natural or synthetic auxins. The affinity for each (synthetic) auxin and co-receptor has not been elucidated yet.

The *Arabidopsis* genome encodes 22 full-length ARFs and three of partial length, (Guilfoyle and Hagen, 2007). The full length ARFs consist of different functional protein domains, including a B3 DNA-binding domain (DBD) and a middle domain that through its amino acid sequence determines whether an ARF acts as a repressor or activator. Based on promoter reporter assays in protoplasts, five *Arabidopsis* ARFs (ARF5-8 and ARF19) were identified as transcriptional activators and the remaining ARFs as transcriptional repressors (Tiwari et al., 2003). The transcriptionally activating ARFs possess an glutamine-enriched middle region that acts as activation domain (AD), whereas repressing ARFs have P,S, and T rich middle region that in some ARFs even contains an EAR repression domain (RD). Recent research revealed extra domains, two dimerization domains (DDs) flanking the DBD, and a Tudor-like ancillary domain in the C-terminal region of the flanking domain (FD). Tudor domains have been shown to bind methylated histones but the methylated domain is lacking in ARFs and thus its function remains unknown (Guilfoyle, 2015; Wright and Nemhauser, 2015; Adams-Cioaba et al., 2012). The DDs facilitate binding of ARFs as dimers to the AuxREs. The ARF - AuxRE binding is sequence specific and multiple motifs have been identified, from which the generic TGTCTC sequence was deduced that has been used to generate the *DR5* promoter that is abundantly used to monitor auxin responses

in plants (Ulmasov et al., 1997) and the more recently discovered specific TGTCGG (Boer et al., 2014).

Four of the activating ARFs can be grouped in sister pairs based on structural- and functional-similarities. The ARF6/8 pair is involved in growth, anther maturation and fruit initiation, and the ARF7/19 pair in lateral root initiation (Okushima et al., 2005; Guilfoyle and Hagen, 2007).

The large diversity in ARFs and Aux/IAAs combined with TIR/AFBs can result in a huge array of diverse, yet specific auxin responses. In total, 6 TIR1/AFBs, 29 Aux/IAAs and 23 ARFs can lead to 4002 hypothetical different auxin responses, which in turn will result in a different onset or attenuation of auxin responsive genes. In addition, expression of auxin responsive genes can be dependent on the degradation dynamics of Aux/IAAs, as was recently shown for IAA14 (Guseman et al., 2015).

The complexity of the mechanism by which different auxin response modules act to coordinate plant development is well illustrated by lateral root development. IAA28 has been described to specify lateral root (LR) founder cell identity and LR initiation is then induced by the SOLITARY ROOT (SLR) /IAA14 – ARF719 module (Fukaki et al., 2002, 2005). Together with the downstream BODENLOSS (BDL)/IAA12 -MONOPTEROS (MP)/ARF5 module it regulates lateral root initiation by specifying cell fate similar to hypophysis specification during zygotic embryogenesis (De Smet et al., 2010; Rademacher et al., 2012). Emergence of the LR through the outer cell layers of the root is subsequently facilitated by SHORT HYPOCOTYL2 (SHY2)/IAA3 together with auxin influx transporter LIKE- AUX1 3 (LAX3) (Goh et al., 2012; Swarup et al., 2008).

Due to the many possibilities of auxin responses the question arises which specific TIR1/AFBs, Aux/IAAs and ARFs act in concert to initiate SE. Here we used reporter lines to identify which auxin response components are expressed during SE, and subsequently tested loss- and gain-of-function mutants of individual auxin response components in our SE system to verify their involvement in the process. By using the direct SE induction system, we show that the TIR/AFB co-receptors and all *Arabidopsis* activating *ARF* genes are expressed during SE initiation. We also demonstrate that ARF sister pairs *ARF7/19* and *ARF6/8* are required with a specific role for the IAA14- ARF7/19 lateral root module in SE. Based on this we show that 2,4-D induced root callus development can be used as a quick test system to identify candidate genes involved in SE. Based on our results, we propose a mechanism in which *SLR/IAA14*–regulated dynamic auxin responses are required for both lateral root and embryonic founder cell specification starting respectively lateral root and somatic embryo development.

Results

The TIR1/AFB-mediated auxin response is required for SE initiation

To investigate whether the TIR1/AFBs are required for SE, single *Arabidopsis tir1-1, afb1, afb2 and afb3* loss-of-function mutant alleles were tested for the efficiency of SE induction from immature zygotic embryos (IZEs, Chapter 2). In short, IZEs obtained 12 days after pollination were cultured for 14 days on 4.5µM 2,4-D and subsequently transferred to hormone free medium to allow somatic embryos to grow out. IZEs from the mutant alleles did not show a significantly different SE efficiency compared to wild-type IZEs (Figure S1), which is probably due to genetic redundancy (Parry et al., 2009). Using translational GUS reporters we explored the expression of *TIR1*, *AFB1*, *AFB2* and *AFB3* during SE (Parry et al., 2009, Figure 1). Interestingly, *TIR1* and *AFB2* showed specific differential expression at the base of the cotyledons, the sites where somatic embryos (SEs) mostly occurred in our SE system, with no or only very weak expression on days 0 and 3, and a significantly increased expression on days 5 and 7 after the start of incubation. *AFB1* also showed enhanced expression at sites of SE initiation, but its expression in IZEs was already relatively high at day 0 and 3. Morphological defects in flower and silique development of triple and quadruple *tir1/afb* mutant plants prevented the availability and use of IZEs from these mutant lines. To overcome TIR1/AFB redundancy and circumvent the morphological defects, we blocked TIR1/AFB-mediated signalling by applying the auxin antagonist auxinole (Hayashi et al., 2012, 2008). Immediate treatment of IZEs with 50 or 100µM auxinole resulted in death of the IZEs (Figure 2a, e, Table S1). IZEs that were pre-induced on SEIM for 3 or 5 days before transfer to SEIM plates supplemented with 100µM auxinole for respectively 11 or 9 days also mostly died (Figure 2a, d, g), whereas transfer to medium with 50µM auxinole resulted in viable IZEs that showed a significant decrease in SE efficiency (Figure 2a, c, f, Table S1). Surviving auxinole-treated IZEs formed white callus from which root and shoot structures regenerated (Figure 2c, d, f, g). Simultaneous analysis of the embryonic cell fate reporter *pWOX2::NLS-YFP* (Breuninger et al., 2008) and the *DR5::RFP* auxin response reporter showed that in IZEs that were induced for 3 days on SEIM and were subsequently treated for 48hr with 100µM auxinole the expression of the reporters was comparable to that in IZEs incubated on hormone free medium (Figure 2h-j). These results showed that the 2,4-D-triggered TIR1/AFB-mediated auxine response is required for IZE survival on SEIM medium as well as for the 2,4-D induced auxin response that triggers SE.

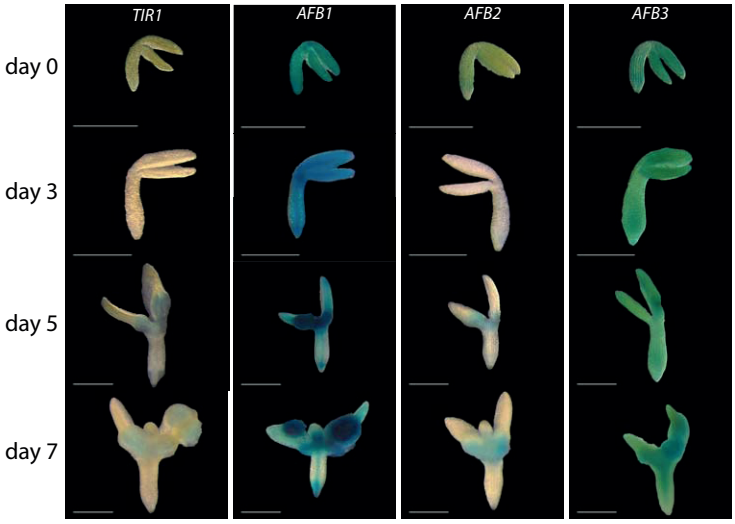

FIGURE 1 - *TIR1/AFB* genes are expressed during *Arabidopsis* SE initiation.
Expression of *TIR1/AFB* genes in IZEs after 0, 3, 5 and 7 days incubation on SEIM, as reported by translational *pTIR1::TIR1-GUS*, *pAFB1::cAFB1-GUS*, *pAFB2::cAFB2-GUS* and *pAFB3::cAFB3-GUS* fusions, Representative images are shown (n=30). Scale bar is 500µm. Please note that for presentation purposes the original background of the IZE images was removed and replaced by a black background.

The activating ARF sister-pairs ARF6/8 and ARF7/19 are involved in SE initiation

Since the auxin response observed during SE initiation must be mediated by activating *ARFs*, we used corresponding promoter-GFP fusions to see which of the corresponding *ARF* genes were expressed and induced in the relevant regions during SE initiation (Figure 3). This analysis showed that, surprisingly, the expression of all five activating *ARF* genes was expressed during SE initiation, and that all five *ARF* genes were expressed at day 7 in the proximal side of the cotyledon where SEs arose. *ARF5* (Figure 3a,d) and *ARF6* (Figure 3b,e) were expressed in the entire IZE on day 5 and day 7, whereas *ARF8* was only expressed in a few cells in the basal and proximal site of the cotyledons of the IZE (Figure 3c,f). *ARF7* expression started at day 7 in the cotyledons and in callus developing on the cotyledons (Figure 3g-j). *ARF19* was expressed in a few cells in the cotyledons and in the proximal area of the cotyledons on day 5 (Figure 3k-n). Results are summarized in a schematic representation of the IZE after 5 and 7 days of SEIM culture (Figure 3o).

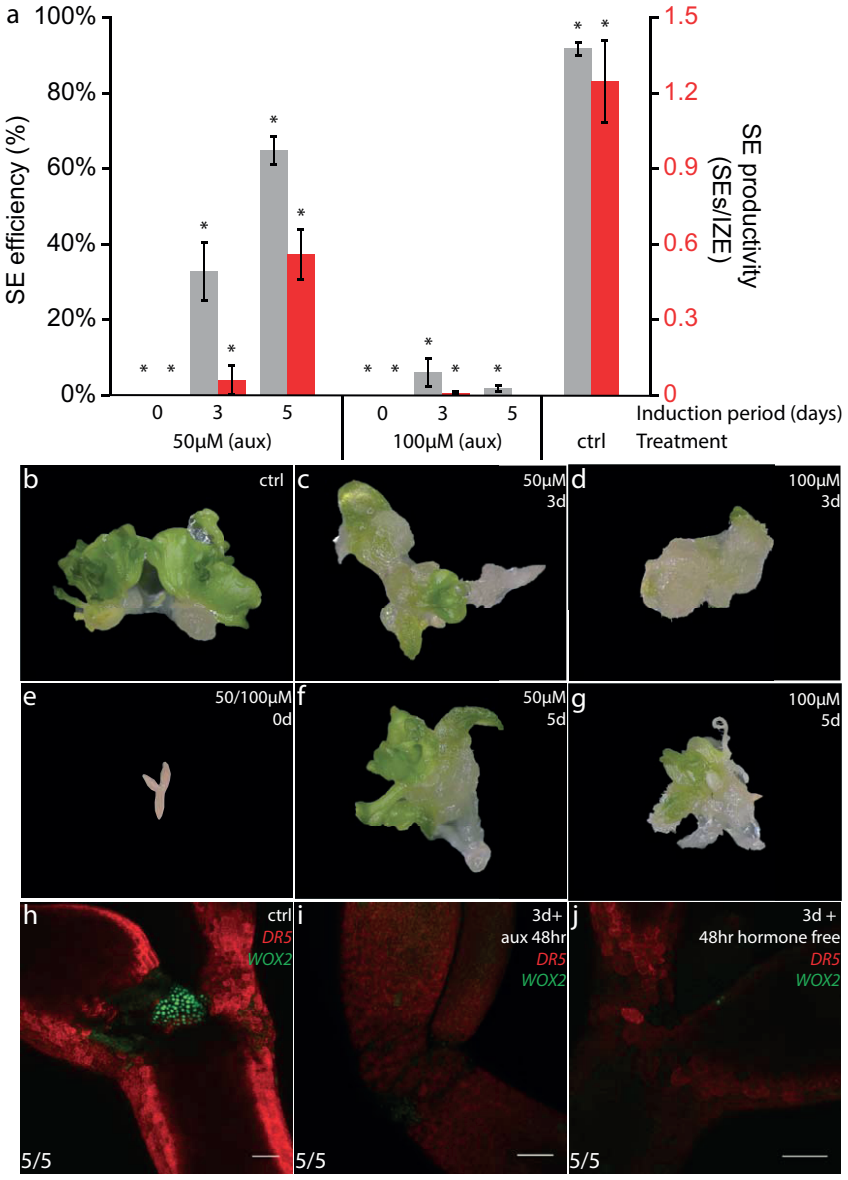

FIGURE 2 - TIR1/AFB-mediated auxin signalling is essential for SE initiation in *Arabidopsis* IZEs.
a) SE efficiency (grey bars) and -productivity (red bars) for control (ctrl) and auxinole (50µM and 100µM) treatments. Bars represent averages of duplo experiments (n=48 per experiment) with the SEM indicated by error bars, * denotes statistical difference between control (ctrl) and treatment (χ^2-test, $p<0.05$ for SE efficiencies, and Welch *t*-test, $p<0.05$ for SE productivities). b-g) Representative phenotypes of IZEs following control (b, ctrl), or 50µM (c,f) and 100µM (d,g) auxinole treatment after 0 (e), 3 (c,d), or 5 (f,g) days of pre-incubation on SEIM. h-j)) Representative confocal images of the SAM and cotyledons of *pWOX2::NLS-YFP DR5::RFP* IZEs incubated on SEIM for 5 days (h, ctrl),or for an additional 48hr on SEIM with 100µM auxinole (i, SEIM) or on hormone free medium (j). Scale bar is 50µm.

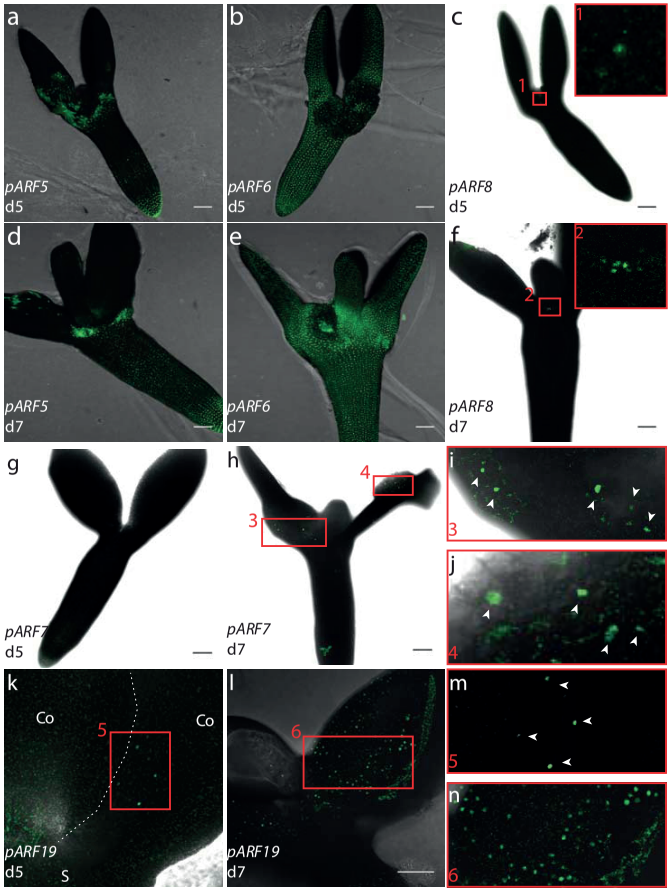

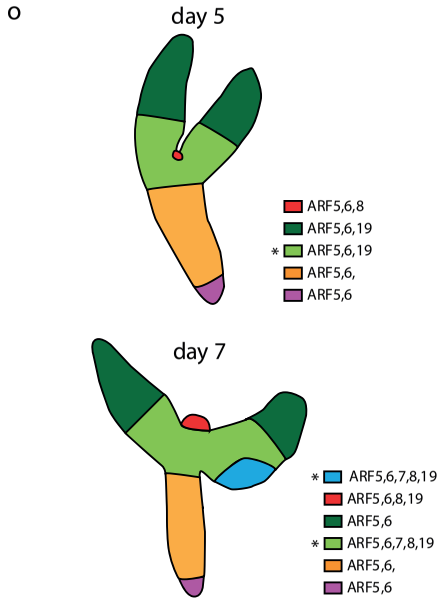

FIGURE 3 - The expression of all five *Arabidopsis* genes encoding activating *ARFs* is enhanced during 2,4-D induced SE initiation.

a-n) Representative CSLM images showing *pARF5::3nGFP* (a,d), *pARF6::3nGFP* (b,e), *pARF8::3nGFP* (c,f), *pARF7::3nGFP* (g-j), and *pARF19::3nGFP* (k-n) IZEs on day 5 (a-c, g, k, m) and day 7 (d-f, h-j, l, n) of culture on SEIM. Red-boxed images in (c) and (f) are magnifications of the regions in boxes (1) and (2), those in (i) and (j) are magnifications of boxes 3 and 4 in (h), and those in (m) and (n) are magnifications of boxes 5 and 6 in (k) and (l), respectively. Scale bar is 100µm, 10-20 IZEs were analysed per timepoint. Dashed lines outline the IZE, Co = cotyledon and S = Sam, arrowheads point towards nuclear GFP. o) Schematic representation of the spatial expression of the indicated ARF genes in IZEs after 5 or 7 days on SEIM. Asterisks indicate regions of SE initiation.

Subsequently, we analysed the SE efficiency of the corresponding T-DNA insertion mutants. A single mutation of *arf6-1* did not result in decreased SE efficiency (Figure 4a) and because of the sterile phenotype of the *arf6 arf8* double mutant we decided to specifically suppress *ARF6* and *ARF8* expression in the embryo by expressing miRNA167 (Wu et al., 2006) under control of the cell division-specific *RPS5A* promoter using a GAL4-*UAS* promoter transactivation system (Weijers et al., 2001). Emasculated flowers of the *Arabidopsis* line *UAS::miRNA167a* were pollinated with *RPS5A::GAL4* pollen. The resulting F1 *RPS5A>>miRNA167a* IZEs showed a significant reduction in the SE efficiency (55%, Figure 4a,b) compared to wild-type IZEs (90%, Figure 4a,c).

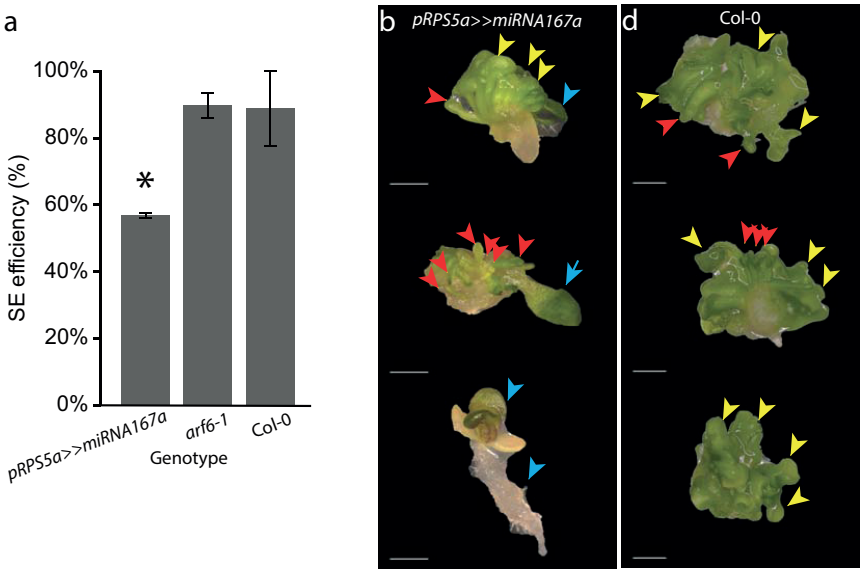

FIGURE 4 - ARF activators ARF6 and ARF8 are both required for SE initiation.
a) SE efficiencies for silenced ARF6/8 by *pRPS5a>>miRNA167a* in F1, *arf6-1* and Col-0 IZEs after standard SE culture. Bars represent averages of duplo experiments (n=48 per experiment) with the SEM indicated by error bars, * denotes statistical difference between control (ctrl) and treatment (χ^2-test, $p<0.05$ for SE efficiencies. b) Representative phenotype images of *pRPS5a>>miRNA167a* and Col-0 IZEs are shown. Root/shoot tissue is indicated with blue arrowheads, embryogenic tissue with yellow arrowheads and individual somatic embryos with red arrowheads, scale bar is 1mm. Please note that for presentation purposes the original background of the IZE images was removed and replaced by a black background.

Two different double mutant combinations were used to study the role of *ARF7* and *ARF19* in SE. Both *arf7-1 arf19-1* and *arf7-1 arf19-2* IZEs showed a significant reduction in SE development compared to wild-type IZEs (Figure 5a). Double mutant IZEs varied in phenotype after SEIM incubation, ranging from IZEs with anthocyanin accumulation in the cotyledons that produced white callus

(Figure 5b), IZEs that started germinating based on cotyledon development and produced callus (Figure 5c), and IZEs that produced somatic embryos (Figure 5d). In general, the *arf7 arf19* double mutant IZEs produced smaller calli and developed more roots and shoots compared to wild-type IZEs (Figure 5e-g). Expression of the auxin response reporter *DR5::RFP* was significantly reduced in the *arf7-1 arf19-1* double mutant compared to wild-type IZEs (Figure 5h-k). Simultaneously, the embryo cell fate reporter *pWOX2::NLS-YFP* in *arf7-1 arf19-1* double mutant IZEs showed reduced expression in the base of the cotyledons (Figure 5o), but stronger expression in the root-hypocotyl junction (Figure 5r) compared to wild-type IZEs (Figure 5n, q). This *pWOX2::NLS-YFP* expression pattern was similar to what was observed in wild-type IZEs incubated on hormone free media (Figure 5l, m, p, s).

In Chapters 2 and 3 we showed that an elevated auxin response followed by a local minimum is first required in the cotyledons of the IZEs to induce SE as marked by *WOX2::NLS-YFP* expression. Our findings here suggest that *ARF7* and *ARF19* are responsible for the overall auxin response induction that represses the embryo fate in the hypocotyl, and is probably required for SE initiation in the cotyledons in regions with a moderate auxin response.

The SLR/IAA14 - ARF7/19 lateral root module is important for SE initiation.

ARF7 and *ARF19* are well known to function together with *SLR/IAA14* during lateral root initiation, and to check whether *SLR/IAA14* is also involved in SE initiation, we analysed the *iaa14-1* loss-of-function allele, the semi-dominant *slr-1* allele that expresses a stabilized version of the SLR/IAA14 protein (Fukaki et al., 2002), and an intragenic suppressor of this allele (*slr-1R1*). Both *iaa14-1* and *slr-1R1* showed wild-type SE efficiencies (80%), whereas the SE efficiency was significantly decreased (10%) for *slr-1* mutant IZEs, which mostly produced white callus with only a few protuberances (Figure 6a,b). Additionally, we analysed *SLR/IAA14* expression using the *pIAA14::GUS* and *pIAA14::mIAA14:GFP* reporter lines, with the latter one expressing a stabilized version of the IAA14-GFP fusion protein (Fukaki et al., 2002). Both reporters showed that the expression of the *IAA14* gene is specifically upregulated on day 7 at the proximal side of the cotyledons, the tissue where SE is initiated in regions of moderate auxin response (Figure 6f-i). The analysis of the mutant alleles indicated that a degradable IAA14 protein is a prerequisite for SE initiation. However, the induction of *IAA14* expression at the site of SE initiation suggested that IAA14 may possibly be required to generate regions of moderate auxin response.

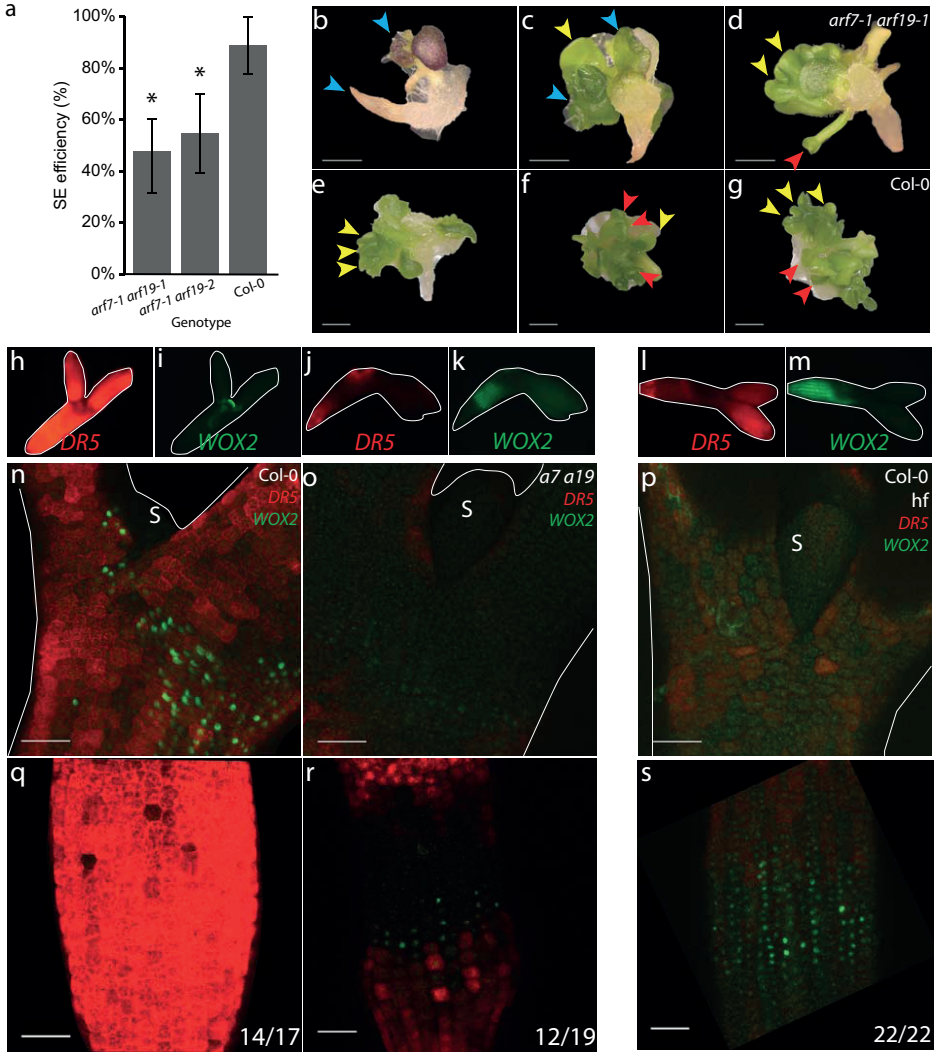

FIGURE 5 - *ARF7/ARF19*-mediated auxin response required for SE initiation in *Arabidopsis* IZEs.

a) SE efficiencies for *arf7-1 arf19-1*, *arf7-1 arf19-2* and Col-0. Bars represent averages of duplo experiments (n=48 per experiment) with the SEM indicated by error bars, * denotes statistical difference between control and treatment (χ^2-test, p<0.05 for SE efficiencies, and Welch *t*-test, p<0.05 for SE productivities). b-g) Representative images of *arf7-1 arf19-1* (b-d) and Col-0 (e-g) IZEs after SE culture, with root/shoot tissue (blue arrowheads), embryogenic tissue (yellow arrowheads) and individual somatic embryos (red arrowheads) indicated, scale bar is 1mm. h-s) Representative CSLM images of *pWOX2::NLS-YFP DR5::RFP* IZEs in Col-0 (h,i,n,q) or *arf7-1 arf19-1* (j,k,o,r) background. in base of cotyledons (n,o) and root-hypocotyl junction (q,r) after 5 days SEIM culture. (l,m,p,s) Col-0 induced for 3 days on SEIM followed by 48hr hormone free (hf) treatment in cotyledons (p) and root-hypocotyl junction (s). Scale bar is 50µm, observation frequencies are indicated in the bottom right corner of (n-s).

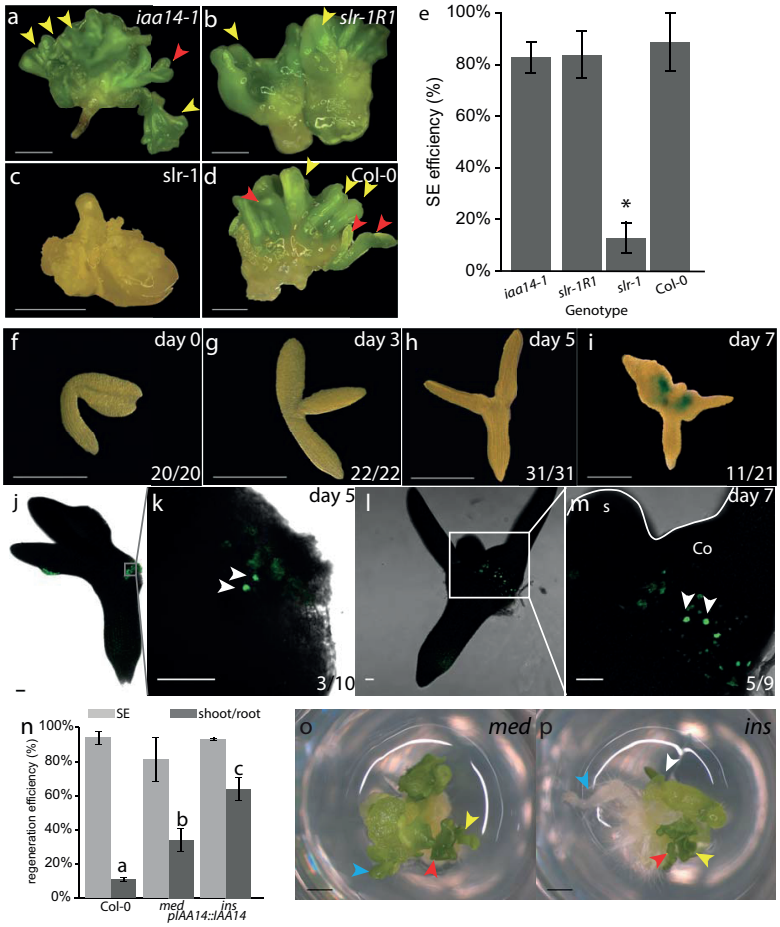

FIGURE 6 - Auxin-induced SE initiation in *Arabidopsis* IZEs requires the expression of auxin-degradable SLR/IAA14.
a-d) Representative images of *iaa14-1* (a), *slr-1R1* (b), *slr-1* (c), and Col-0 (d) IZEs after standard SE culture, scale bar is 1mm. e) SE efficiencies for *iaa14-1*, *slr-1R1* and *slr-1* mutant alleles and Col-0. Bars represent averages of duplo experiments (n=48 per experiment) with the SEM indicated by error bars, * denotes statistical difference between control and treatment (χ2-test, $p<0.05$ for SE efficiencies, and Welch *t*-test, $p<0.05$ for SE productivities). f-i) GUS stained *pIAA14::GUS* IZEs after 0, 3, 5, 7 days in SEIM culture, n=20-31 IZEs per timepoint. Scale bar indicates 500µm, observation frequencies are indicated in the bottom right corner. j-m) GFP signal in *pIAA14::mIAA14-GFP* after 5 days (j,k) and 7 days (l,m) in SEIM culture. Scale bar indicates 50µm, observation frequencies are indicated in the bottom right corner, S = SAM, Co = cotyledon. White arrowheads point at *pIAA14::mIAA14-GFP* expression. n) Regeneration efficiencies of *pIAA14::IAA14 medium (med)* and *pIAA14::IAA14 insensitive* (ins) IZEs. Light grey bars indicate the SE efficiency, and dark grey bars indicate the shoot/root regeneration efficiency. Bars represent averages of duplo experiments (n=48 per experiment) with the SEM indicated by error bars, letters denote statistical difference between control and med (a,b), control and ins (a,c), med and ins (b,c) (χ2-test, $p<0.05$ for SE efficiencies). o,p) Representative images of *pIAA14::IAA14 med* and *ins* IZEs after standard SE culture. Arrowheads in a-d) and o,p) indicate root/shoot tissue (blue arrowheads), embryogenic tissue (yellow arrow heads) and individual somatic embryos (red arrowheads), scale bar is 1mm. Please note that for presentation purposes the original background of the IZE images in (a-d, f-i) was removed and replaced by a black background.

Previously, it was shown that the Aux/IAA turnover rate determines the pace of an auxin-regulated developmental process such as lateral root formation (Guseman et al., 2015). The turnover rate of Aux/IAAs is dependent on the degradation rate of the protein, which can be influenced by the stability of the protein structure (Guseman et al., 2015), by the type of auxin present and its concentration, and by its affinity for the specific TIR1/AFB co-receptors present in the cell (Calderón Villalobos et al., 2012; Lee et al., 2014). The stability of the Aux/IAA proteins is largely dependent on the degron domain DII. To test whether the turnover rate of IAA14 played a role in SE initiation we analysed IZEs expressing mutated versions of IAA14, respectively medium (*iaa14med*) and insensitive (*iaa14ins*) under control of their native *IAA14* promoter (Guseman et al., 2015). The *iaa14med* version has a point mutation changing glycine to glutamic acid in the 72nd position of the DII domain (G72E) and the *iaa14ins* version contains a substitution changing proline to serine in the 81st position of the DII domain (P81S), which is comparable to the original *slr-1* mutation (P82S) (Fukaki et al., 2002; Guseman et al., 2015). Surprisingly, we observed wild-type SE efficiencies for both mutant lines (80-90%), but a significant increase in the shoot/root regeneration efficiency for *iaa14med* (34%) and *iaa14ins* (64%) IZEs compared to wild-type IZEs (11%) (Figure 6n-p). The discrepancy with the original *slr-1* mutation might be explained by the fact that no wild-type IAA14 protein is present in the *slr-1* mutant and that the *slr-1* mutant protein is expressed from its native promoter, whereas the expression of *iaa14med* and *iaa14ins* is controlled by a 2kb *IAA14* promoter region that is inserted at another location of the genome of wild-type *Arabidopsis*. Although this was sufficient to repress lateral root development, the *iaa14ins* line did not fully mimic the *slr-1* SE deficient phenotype (Figure S2, S3), and possibly the *iaa14ins* construct under the IAA14 promoter is not sufficiently expressed in IZEs to significantly reduce the SE efficiency (Fukaki et al., 2002).
Still, the enhanced organogenesis observed in the *iaa14med* and *iaa14ins* lines correlated nicely with the stability of the mutant proteins, and the steep reduction in SE efficiency with *slr-1* mutant IZEs suggests that the regeneration process can be modulated by repression of the auxin response, with weak repression leading to organogenesis, and strong repression to callus formation.

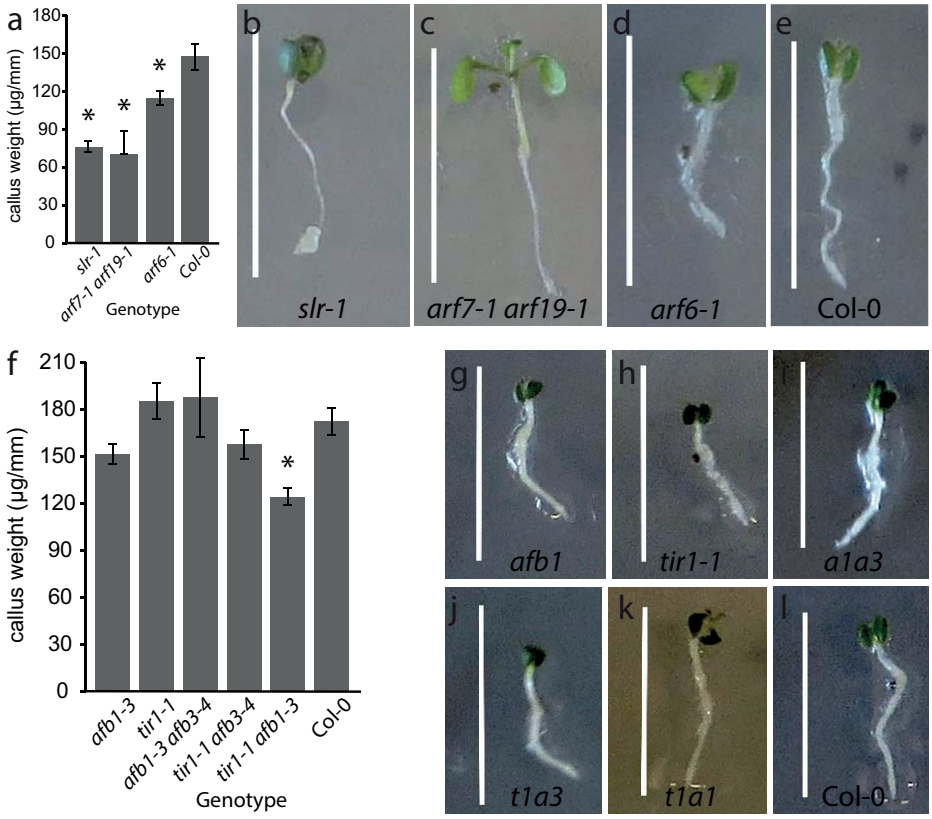

FIGURE 7 - Auxin-induced root callus development as a phenotypic screen for *Arabidopsis* mutants defective in SE.
a, f) Quantification of weight per mm root length for the *slr-1*, *arf7-1 arf19-1*, *arf6-1* mutants (a) and several single and double *tir1/afb* mutants (f) after incubation for 4 days on hormone free medium followed by 4 days on SEIM. Bars represent averages of a single experiment (n=35-50), with the SEM indicated by errors bars.* denotes statistical differences between a mutant line and wild-type Col-0 (Welch *t*-test, $p<0.05$) b-e, g-l) Representative images of *slr-1* (b) *arf7-1 arf19-1* (c) *arf6-1* (d) *afb1-3* (g) *tir1-1* (h) *afb1-3 afb3-4* (i), *tir1-1 afb3-4* (j) *tir1-1 afb1-3* (k) and Col-0 (l). Scale bar is 1cm.

Root callus formation as an easy phenotypic pre-screen to identify candidate genes involved in SE initiation

To determine the SE efficiency for many different *Arabidopsis* mutant backgrounds is a time-consuming, laborious process, because it requires the availability of fertile flowering plants (which is problematic for several important mutant backgrounds) and accurate timing of manual emasculation, pollination of flowers and harvesting of the IZEs from the ovules. In this chapter we showed that lateral root deficient mutants were impaired in SE. In addition, several groups have shown that lateral root deficient mutants are defective in 2,4-D-induced

root callus development (DiDonato et al., 2004; Sugimoto et al., 2010; Fan et al., 2012). This together with the involvement of the IAA14-ARF7/19 auxin signalling module in SE initiation suggested strong similarities between root callus development and lateral root- and SE initiation. We therefore tested whether besides lateral root initiation also 2,4-D-induced root callus development could be used as an easy pre-screen to identify candidate genes involved in SE initiation.

For our experiments we used the SE and lateral root deficient mutants *slr-1* and *arf7 arf19* as a negative control and Col-0 and the single *arf6-1*, *tir1-1* and *afb1*-1 mutants as a positive control (no effect on SE initiation). Furthermore, we tested the *afb1-3 afb3-4* and *tir1-1 afb3-4* double mutants, as based on the strong effect of auxinole on IZE survival and SE imitation we expected to see an effect here on callus development. Four days old seedlings grown on hormone free medium were transferred to SEIM and after four days the shoot was removed, weight and length of the remaining hypocotyl and root was measured and the weight per mm root length was calculated for 35-50 seedlings per genotype. Matching with our expectations, *slr-1* and *arf7-1 arf19-1* seedlings showed a significant reduction in root callus development as compared to wild-type seedlings (Figure 7a). In *slr-1* seedlings callus development was restricted to the root tip, whereas in *arf7-1 arf19-1* seedlings callus development was reduced over the entire root length (Figure 7b) compared to wild-type seedlings (Figure 7e). Unexpectedly, *arf6-1* also showed a significant reduction in the weight per mm root (Figure 7d), whereas no effect on lateral root initiation (Figure S4) or SE initiation was observed. The role of the ARF6/8 pair in both lateral and adventitious root initiation is well described (De Rybel et al., 2010; Gutierrez et al., 2012). From this we concluded that 2,4-D-induced root callus formation might be a more sensitive method to assess the involvement of a gene in SE or lateral root initiation.

Similar to our results for SE initiation (Figure S1), the *tir1-1* and *afb1-3* single and the *afb1-3 afb3-4* double mutants did not affect root callus development. However, the double *tir1-1 afb1-3* did show a significantly reduced callus weight per mm compared to Col-0. Although we have not tested this double mutant for SE initiation, our results are in line with the auxinole inhibitor experiments, and thus corroborate the redundant action of the TIR1/AFBs during SE initiation. These results suggest that root callus development can be used as a relatively easy and quick pre-screen to identify candidate genes involved in SE. A major advantage of this system is that it allows testing of mutants that due to fertility problems do not produce homozygous mutant embryos and it reduces time from nine weeks to 8 days to get the first indication for candidate genes involved in SE initiation.

Discussion

In contrast to the natural auxin IAA or other auxin-like compounds, only the synthetic auxin 2,4-D is able to induce SE in various plant species using specific tissues as explants. A general molecular pathway has been elucidated for auxins, yet specificity for each type of auxin remains to be elucidated. Auxin is perceived in plant cells by TIR1/AFB – Aux/IAA co-receptor pairs, which lead to the degradation of the Aux/IAA repressor proteins and the subsequent activation of auxin responsive gene expression by derepression of the activating ARFs that formed heterodimers with the degraded Aux/IAA protein. Here we investigated which auxin signalling components are specifically involved in 2,4-D-induced SE on *Arabidopsis* IZEs.

SE is dependent on TIR1/AFB mediated signalling

In this chapter we showed by using the auxin antagonist auxinole that TIR1/AFB signaling is important for IZE survival on SEIM and for SE initiation. GUS reporter expression analysis showed that all TIR1/AFBs are expressed in the IZE during SE initiation, and that specifically the expression of *TIR1* and *AFB2* is induced in the tissues that form SEs. Our results are in line with the recent report that *miR393*-mediated repression of *TIR1/AFB* expression leads to reduced SE efficiencies (Wójcik and Gaj (2016). In contrast to our results, however, Wojick and Gaj (2016) found a significant reduction in the SE efficiency and productivity in the *tir1-1* and *afb2-3* single mutants, whereas in our hands the same single mutant alleles were not significantly affected. In fact, Wojick and Gaj (2016) reported that the effect of the single mutant alleles is similar or even stronger than that of *miR393* overexpression. Although this result seems quite counterintuitive, since *miR393* overexpression is expected to target *TIR1*, *AFB2* and *AFB3* genes, it might relate to the weak phenotypes that were previously reported for the *miR393* overexpression lines (Parry et al., 2009). The different results obtained with the *tir1-1* and *afb2-3* single mutants are likely to be due to differences in the methodology of IZE selection for the experiments and how the SE efficiency was scored. Based on the gene expression pattern and the root callus induction assay, we did identify the involvement of *TIR1*, *AFB1* and *AFB2* in SE initiation. Because of their strong functional redundancy, it will however be difficult to disentangle the role of each individual *TIR1/AFB* gene in the SE initiation process.

Lateral root formation and SE initiation share auxin signalling components

When looking at auxin signalling components downstream of the TIR1/AFBs, we found to our surprise that all activating *ARFs* (5,6,7,8 and 19) were expressed in

2,4-D treated IZEs at the base of the cotyledons, the sites where SEs mostly occur during SE induction. Unfortunately, our experimental system did not allow to analyse the effect of some of the corresponding mutants, as either homozygous mutant embryos were defective and could not be grown to flowering plants producing viable IZEs (*mp/arf5*, Hardtke and Berleth, 1998), or the homozygous plants were completely sterile (*arf6 arf8,* Nagpal et al., 2005). The role of the *ARF6/ ARF8* gene pair could however be assessed by down regulating their expression using *miRNA167a* overexpression under the control of the *RPS5a* promoter (Wu et al., 2006; Weijers et al., 2001). Generated F1 *RPS5a>>miRNA167a* IZEs showed significantly reduced SE efficiencies, and since the single *arf6-1* mutant did not show this reduction, it is likely that *ARF6* and *ARF8* function redundantly in the SE initiation process, similar to their redundant role in anther dehiscence (Nagpal et al., 2005) or adventitious root formation (Gutierrez et al., 2009). Recently, the importance of *ARF6* and *ARF8* was also shown for a secondary SE system in liquid medium (Su et al., 2016).

For the other activating *ARF* pair *ARF7/19* mutant embryos could be tested, because both *arf7-1 arf19-1* and *arf7-1 arf19-2* double mutant did not lead to embryo lethality or infertility. Interestingly, both *arf7 arf19* double loss-of-function mutants showed a significant reduction in SE efficiency from 90% to 50%. *ARF7* and *ARF19* act in lateral root initiation together with *SLR/IAA14* (Fukaki et al., 2002, 2005), and when we tested IZEs of the semi-dominant *slr-1* allele encoding a stabilized version of the SLR protein they showed an even stronger strong reduction in the SE efficiency (10%) compared to the *arf7 arf19* double mutant IZEs. This suggests that the SLR/IAA14 protein may also repress other activating ARFs involved in SE initiation. A recent study on Aux/IAA - ARF interactions has indeed shown that SLR/IAA14 can interact with all activating ARFs, including ARF6 and ARF8 (Piya et al., 2014). This then makes it likely that both ARF7/19 and ARF6/8 pairs are involved in SE initiation, and that SLR/IAA14 is the central Aux/IAA regulating this process. The induction of *pIAA14::GUS* expression in the same region where SEs are formed is in line with its role as modulator of auxin response during SE initiation. By simultaneous analysis of the auxin response and embryo cell fate in the *arf7 arf19* background, we showed that an *ARF7/ ARF19*-dependent elevated auxin response is required to suppress embryo cell fate identity in the IZE, and that this subsequently leads to the generation of regions with a reduced auxin response where somatic embryos are initiated. Interestingly, such an auxin response minimum was also reported during LR founder cell specification (Dubrovsky et al., 2011). The coinciding upregulation of IAA14 expression make it tempting to speculate that this Aux/IAA is possibly

involved in generating regions of reduced auxin response where SEs are initiated.

A common model for LR and SE founder cell specification and start of development

Based on our observations and the similarities between the lateral root and SE pathway we propose a model in which an overall elevated auxin response activated by TIR1, AFB1 and AFB2 and mediated by ARF7/19 (and possibly ARF6/8) is required to reset the specified cell fate in both LR and SE systems. Our finding that an elevated auxin response was absent in the *arf7 arf19* background during SE initiation supports this hypothesis. Generation of a subsequent auxin response minimum, possibly assisted by enhanced SLR/IAA14 expression or stability, defines a developmental window for either LR or SE founder cell specification followed by the first cell division that respectively marks LR- or SE initiation (Figure 8). Interestingly, in both the zygote and lateral root founder cells a lowering and localized auxin response is required to undergo an asymmetric cell division (Scheres et al., 1994; Swarup et al., 2008; Robert et al., 2013; Yoshida et al., 2014), but whether SE starts with a similar asymmetric cell division and auxin distribution remains to be shown. Our results and those of Gliwicka et al. (2013) showed that also *ARF5* is expressed during SE, however a role for this this gene could not be established in our study. We propose that *ARF5* fulfils a similar role as in LR initiation and development, in which the *IAA12/BDL – ARF5* module acts downstream of *IAA14 – ARF7/ARF19*, where similar to its role during zygotic embryogenesis the IAA12/13 – ARF5 module might be involved in specification of the hypophysis (Weijers et al., 2006; Schlereth et al., 2010) and the provascular tissue (Hardtke and Berleth, 1998) in the somatic embryo. Experiments in which a non-repressible *ARF5* (Krogan et al., 2012) is introduced into the semi-dominant *slr* mutant could possibly reveal whether *ARF5* plays a role in SE initiation or that it rather is involved in downstream processes. Moreover, a non-repressible *ARF7* or *ARF19* could possibly reveal the importance of SLR/IAA14 in generating the regions of reduced auxin response in which SE is initiated.

In summary, our results show that lateral root initiation is similar to SE initiation in that an auxin maximum followed by a minimum is required to initiate SE or lateral root development, and the auxin responses in both systems are modulated by the same SLR/IAA14-controlled module. Based on this similarity we propose that the 2,4-D root callus induction assay (DiDonato et al., 2004; Sugimoto et al., 2010; Fan et al., 2012) could be used as a relatively quick phenotypic screen, as a first step in identifying gene candidates involved in SE.

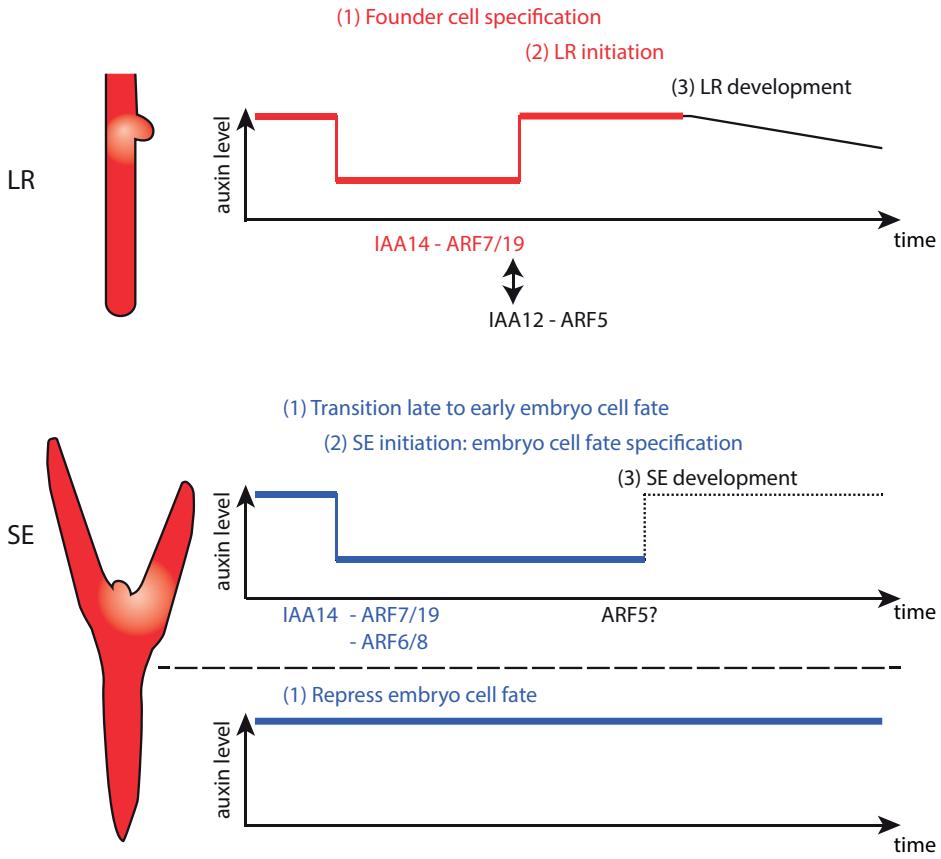

FIGURE 8 - Model for the involvement of auxin and auxin signalling components in lateral root and somatic embryogenesis initiation.

An initial auxin response maximum involving ARF7/19 and possibly also ARF6/8 is required to induce cell reprogramming, after which local auxin response minima in the root pericycle or IZE epidermis specify the lateral root or embryonic founder cells. Possibly, the enhanced expression of IAA14 is responsible for these transient local auxin minima by repressing the activity of ARF7/19 and possibly also ARF6/8. Subsequent degradation of the IAA14 repressor allows these activating ARFs to reactivate the auxin response, which triggers (asymmetric) division of the founder cells leading to lateral root (LR) development- or somatic embryogenesis (SE). To initiate LR, a second module IAA12- ARF5/MP is required to trigger the process, and ARF5 is possibly involved in SE as well. After the start of the developmental program, a gradual decrease in auxin levels allows patterning and growth of the developing root. At present, the specific details of the auxin response during SE (dashed line), after SE initiation is not yet known.

Methods

Plant lines and genotyping

All *Arabidopsis thaliana* lines described are in the Columbia (Col-0) background and summarized in Table S3. The *pWOX2::NLS:YFP* line was kindly

donated by Thomas Laux and is resistant to phosphinothricin (ppt) (Breuninger et al., 2008). The *DR5::RFP* line was donated by Eva Benkova and is resistant to hygromycin (hyg) (Marhavý et al., 2011). The collection of kanamycin (kan) resistant *pARFxx::SV40x3GFP* lines was kindly provided by Dolf Weijers (Rademacher et al., 2011). Hidehiro Fukaki donated *slr-1*, *slr-1R1*, *pIAA14::GUS*, and *pIAA14::IAA14m:GFP* (Fukaki et al., 2002). Jennifer Nemhauser kindly provided *pIAA14::IAA14 G79E (iaa14med), pIAA14::IAA14 P81S (iaa14ins)* (Guseman et al., 2015). Jason Reed kindly donated the *UAS::miR167a* line (Wu and Reed, unpublished) and the *pRPS5a::GAL4* was previously described (Weijers et al., 2001). Mark Estelle donated the *tir1-1 afb1-3 afb2-3/+ afb3-4* quadruple mutant from which segregating double mutants were selected, and the *pTIR1::cTIR1-GUS pAFB1::cAFB1-GUS*, *pAFB2::cAFB2-GUS*, and *pAFB3::cAFB3-GUS* reporter lines (Parry et al., 2009). The *iaa14-1* (N25214/CS25214), *arf7-1 arf19-1* (N24629), *arf7-1 arf19-2* (N24630), *arf6-1* (N24606) mutants were obtained from NASC (www.arabidopsis.info) and are described respectively in Overvoorde et al. (2005) and Okushima et al. (2005). Single *tir1-1* (N3798), *afb1-3* (N662878), *afb2-3* (N637151), and *afb3* (N657515) mutant lines were obtained from NASC as well.

Genotyping

Sequences of DNA primers used for genotyping are provided in Table S2, All PCR reactions were performed using DreamTaq DNA polymerase (ThermoFisher Scientific, EP0705) on genomic DNA isolated as described by Giraudat (2003), melting temperature and annealing time was 55°C and 60s, unless otherwise stated.

Plant tissue culture and growth conditions

Arabidopsis seeds were surface sterilized and germinated on MA medium (Masson and Paszkowski, 1992) complemented with 1% (w:v) sucrose, and 0.8% (w:v) Daishin agar, pH5.8. For antibiotic selection ppt, hyg or kan was added to the medium after autoclaving at a final concentration of 20mg/mL for ppt and hyg, and of 50mg/mL for kan. Seven to ten days after germination (dag), seedlings were transferred to a mixture of soil and sand, 2 per pot, and grown under a 16hr. photoperiod and 70% relative humidity. IZEs were harvested from plants 1-2 weeks after flowering. The siliques were surface sterilized with a 20% bleach/70% ethanol solution for 5min. and rinsed at least three times with sterile water.

SE-inducing medium (SEIM) consisted of B5 medium, with 4.5µM 2,4-D, 2% (w:v) sucrose and 0.8% (w:v) Daishin agar (Gaj, 2011; Nowak et al., 2012). Hormone free medium was MA medium (Masson and Paszkowski, 1992). Media were sterilized

by autoclaving at 120°C for 20min. SE was performed in sterile 48-wells plates (Greiner cellstar art. nr. 677180) that were filled with 400µL SEIM or hormone free medium using a repeater pipet. IZEs were placed on SEIM (one per well) and incubated overnight at 4°C in the dark followed by incubation at 21°C under a 16hr photoperiod for a standard period of 14 days, followed by 7 days incubation on hormone free medium (standard SE culture). Auxinole was kindly donated by Ken-Ichiro Hayashi (Hayashi et al., 2008, 2012) and was added to SEIM from a 50mM stock solution in DMSO to final concentrations of 50µM and 100µM.

For the SE efficiency studies with inhibitors or mutant IZEs, IZEs synchronized in their developmental stage were obtained by manual pollination. For this purpose, the 2 or 3 oldest but still closed flower buds of primary inflorescence stems were emasculated and pollinated and 12 days after pollination (dap) IZEs were excised from the ovule using a dissecting microscope. Per two parent plants, 2-3 sets of 2-3 closed flower buds were emasculated.

To keep data comparable between inhibitor experiments, large-scale experiments were set up as follows: the 50µM and 100µM auxinole and 2,4-D control treatments were performed in duplicate for all 2,4-D pre-induction periods (0, 3 and 5 days). Per treatment, 48 IZEs were used, one IZE per well in a 48-wells plate. For the 3 and 5 days induction, a large pool of IZEs was cultured in multiple 48-wells plates. At day 3 and day 5 48 IZEs were selected randomly out of the different plates for each treatment and transferred to plates containing 2,4-D and 100µM inhibitor. For the day 0 treatment 4 siliques were used to compile 1 plate per treatment (12 IZEs per silique).

The mutant studies were performed by culturing 48 IZEs per genotype in duplicates.

For confocal or light microscopy analysis non-synchronized late IZEs from more or less the same developmental stage were selected based on their size as described by (Gaj, 2011). Broken or damaged IZEs were discarded and not used.

Statistics of SE

To quantify SE, four categories were used to score 1) embryogenic tissue (also referred to as embryogenic callus), if no individual somatic embryos were found but embryogenic tissue developed. Embryogenic tissue was defined as smooth green structures without trichomes, that either looked like fused cotyledons or like fused zygotic embryos 2) SE forming IZEs, if individual somatic embryos were observed that were attached to the IZE by their root pole. In that case, the number of individual somatic embryos was counted. 3) Non-embryogenic callus forming IZEs, if callus was formed that remained white-yellowish without

developing somatic embryos or embryogenic tissue 4) Dead IZEs, if the tissue turned white, showed no growth and maintained their original size.

Category 1 and 2 were merged to quantify the number of responding IZEs that produced embryogenic tissue. The SE efficiency was then calculated as (Luo and Koop, 1997)

$$SE\ efficiency = \frac{N_r}{N_t} \quad 100\%$$

N_r = the number of responding explants. N_t = total number of explants tested.

SE productivity was calculated as

$$SE\ productivity = \frac{N_i}{N_t}$$

N_i = the number of individual somatic embryos observed. N_t = the total number of IZEs that were tested (including the ones that died).

Statistics for SE efficiency were performed in Microsoft Excel, using the χ^2-test for association (Holmes et al., 2011). For SE productivity, a Welch *t*-test was performed in Rstudio (Pace, 2015).
For inhibitor studies we compared the control treatments to check whether refreshment of SEIM would contribute to SE efficiency and productivity. The two controls were not statistically different for SE efficiency and productivity (respectively χ^2_{calc}=2.9, and *t*-test p-value 0.524, described in Chapter 2) and for this reason we performed all statistical tests between the treatment and the 0 days control.

Root callus assay

To induce root callus, seeds were germinated and grown on hormone free medium for four days and subsequently transferred to SEIM for another four days. After a total of 8 days culture the plates, including a scale, were photographed with a compact camera Canon PowerShot SX260 HS. The root length was measured using FIJI. To measure root weight, the shoot was removed and the weight of the root, including callus that developed, were measured. The root weight per mm was calculated in Microsoft Excel and the Welch *t*-test in Rstudio was used to calculate statistical differences (Pace, 2015).

GUS staining

Staining for B-glucuronidase (GUS) activity was performed as described by Malamy and Benfey (1997) with the following modifications: The staining solution was made as follows: a K/NaPI buffer was made by adding approximately 50mL 0.5M KH_2PO_4 to 125mL 0.5M Na_2HPO_4 tuntil pH reached 7.0.40mL of this solution was diluted with MilliQ to 200mL, and.subsequently2mL 1M EDTA (pH8.0), 2mL 0.1M $K_4Fe(CN)_6$, 2mL 0.1M ($K_3Fe(CN)_6$ and 200uL 0.1% Triton were added. X-gluc (Duchefa, X1402) was pre-dissolved in DMSO at 100mg/mL and was added to the staining solution at a final concentration of 1mg/mL. The bottle with the solution was wrapped in aluminium foil and stored at 4°C for a maximum of 6 months. Samples were submerged in 1-2mL staining solution and incubated for 3hr at 37°C followed by overnight incubation at room temperature to increase staining. Samples were destained with 0.24M HCL 20% methanol for 15min at 55°C, followed by 15min incubation in 7% (w:v) natriumhydroxide/ 60% ethanol for clearing. Samples were rehydrated through an ethanol series 50% - 30% - 10% - 5%, with 5min incubation between each step. To completely remove chlorophyll from the embryos, samples were then cleared for at least 1hr with a 25% (w:v) chloralhydrate in 50% glycerol solution.

Microscopy

Images of (GUS stained) IZEs were taken with a Leica DC 500 stereomicroscope using the Leica Application Suite v2.8.1 software or a Zeiss Axioplan DIC/Nomarski microscope equipped with Axiocam MRc5 camera and AxioVision40 V4.7.2.0 software and a 10x objective. Image editing was performed in FIJI and Adobe Photoshop CS5.1 and figures were assembled in Adobe Illustrator CS5.1

Confocal Laser Scanning Microscopy (CSLM) was performed with a ZEISS LSM510 exciter equipped with argon and helium/neon lasers. GFP and YFP were detected using a 488nm band pass filter for excitation and a 500-530nm band pass filter for emission. Simultaneously, chlorophyll background fluorescence was captured with a 650nm long pass emission filter. RFP was excited at 530nm and was captured with a 550-600nm band pass emission filter. Images were captured with ZEISS ZEN2009 software.

Fluorescence combined with Differential Interference Contrast (DIC) microscopy was performed with a Zeiss Axioplan DIC/Nomarski microscope equipped with Axiocam MRc5 camera and AxioVision40 V4.7.2.0 software and a 10x objective, red and green filters were used to capture RFP and GFP images, respectively.

Samples were prepared on a microscope slide by embedding IZEs in a thin layer of 0.5% low melting point agarose, and adding a droplet of water before covering with a cover slip.

Acknowledgements

C.P. was supported by an NWO-TTI-Green Genetics core project grant (NWO 828.11.004) to R.O. from the Earth and Life Sciences Division with financial support from the Netherlands Organisation for Scientific Research (NWO). We thank Gerda Lamers for her help with microscopy.

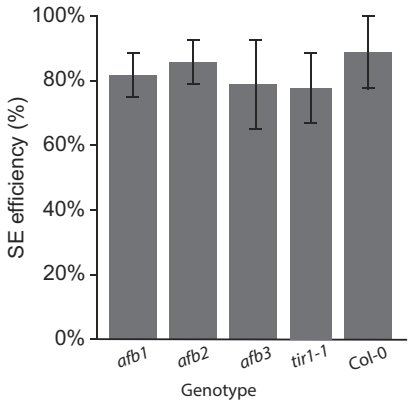

FIGURE S1 - SE efficiencies for single *tir1/afb* mutant and wild-type IZEs. Bars represent duplo experiments (n=48) with the SEM indicated by error bars. No statistical difference was observed between mutant and wild-type IZEs. ($\chi 2$ test , $p<0.05$).

TABLE S1 - Frequency (%) of IZEs not surviving when induced on SEIM supplemented with 50 or 100µm auxinole starting day 3 and 5 in culture. As a control, IZEs cultured on SEIM were included. Frequencies are averages of duplo experiments (n=48 per experiment).

2,4-D induction period (days)	**0**		**3**		**5**		**ctrl**
auxinole (uM)	50	100	50	100	50	100	0
death (%)	100	100	18	90	1	45	0

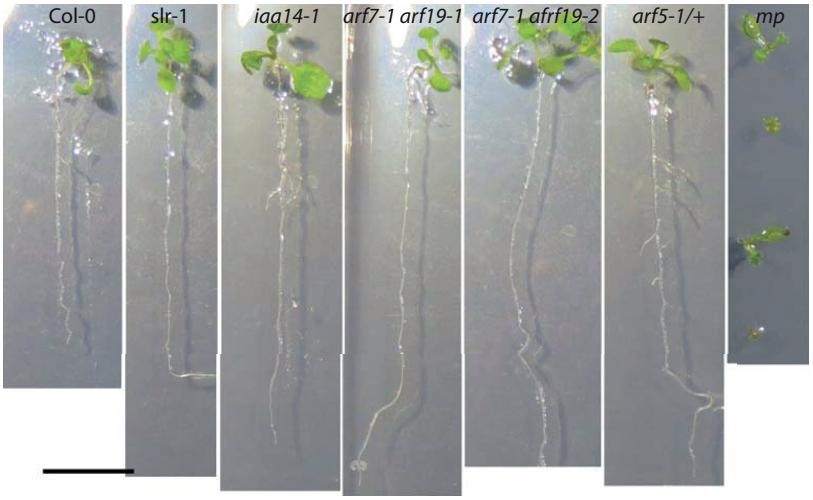

FIGURE S2 - Phenotypes of Col-0, *slr-1*, *iaa14-1*, *arf7-1 arf19-1*, *arf7-1 arf19-2*, *arf5-1/+* and *mp* seedlings germinated and grown for 14 days on hormone free medium. Scale bar is 1cm.

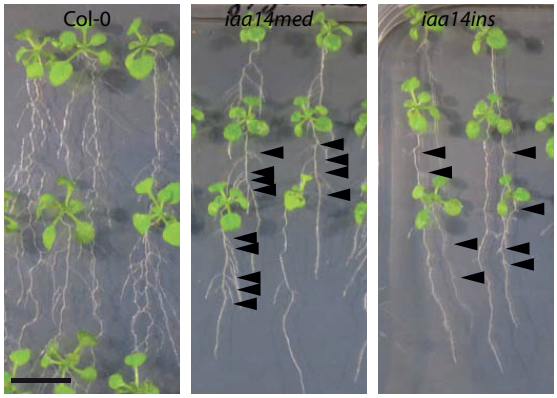

FIGURE S3 - Phenotypes of *iaa14med* (a) *iaa14ins* (b) and Col-0 (c) seedlings germinated and grown for 14 days on hormone free medium. Arrowheads point at lateral roots.. Scale bar is 1cm.

FIGURE S4 - Phenotypes of Col-0 and *arf6*-1. Seedlings were germinated and grown for 10 days on hormone free medium. Scale bar is 1cm.

TABLE S2 - Primers used for genotyping *Arabidopsis* mutant alleles. GSP is gene- specific primer, BP is border-specific primer. All reactions were carried out on genomic DNA, DreamTaq polymerase, Tm = 55ºC, At = 60s, unless otherwise stated.

Gene	Primer orientation	Sequence (5' - 3')	Remarks
arf5-1	GSP left	GAGAGGAAGTAAGCACCCGAC	
	GSP right	TCATTACATCCAGGCTCATCC	
	BP	LBB1.3 salk	
arf6-1	GSP left	GGGAGATTGAGCCTTTAACAACA	Tm=47.9C
	GSP right	TCGCTTCGCAGCTCGTGGTAGCTGCT	
	BP	GAGACATCTCCTTACCACGG	
arf7-1	GSP left	TGCACTCCTCTTTGAACCATC	Tm 58.6C
	GSP right	CACGAGTTCTTGTTTTAGCCG	
	BP	LBB1.3 salk	
arf19-1/arf19-2	GSP left	GTCATATCCAGCGACAGTATG	arf19-1 CP129 + CP124
	GSP right	GAGGTTTGGGGATTGGAAGTTCA	arf19-2 CP128 + CP124
	BP	JMLB1	
***tir1-1* (single)**	GSP left	AGCGACGGTGATTAGGAGGT	CAPS digestion with BsaI
	GSP right	CAGGAACAACGCAGCAAAA	
***afb1-3* (single)**	GSP left	AACGGAAGACTAGGAAGCGAG	SALK_070172
	GSP right	GCAACAGCTTCAAGACCTTTG	
	BP	LBB1.3 salk	
***afb2-3* (single)**	GSP left	TCAACGGTCAAGATCCATCTC	SALK_137151
	GSP right	CTGCAATTAGCGGCAATAGAG	
	BP	LBB1.3 salk	
***afb3* (single)**	GSP left	TGCTTTGCTGATCTTCTAAGG	SALK_016356C
	GSP right	AGGGTCTAAGACGGCTCTCTG	
	BP	LBB1.3 salk	
***tir1-1* (double)**	GSP left	AGCGACGGTGATTAGGAGGT	CAPS digestion with BsaI
	GSP right	CAGGAACAACGCAGCAAAA	
***afb1-3* (double)**	GSP left	GGCGAAAAGTTCGTCTCTTG	SALK_070172
	GSP right	AAGATCAGGCATTCGGACAG	
	BP	LBB1.3 salk	
***afb2-3* (double)**	GSP left	TTCTCCTTCGATCATTGTCAAC	SALK_137151
	GSP right	TAGCGGCAATAGAGGCAAGA	
	BP	LBB1.3 salk	
***afb3-4* (double)**	GSP left	GGGTCTAAGACGGCTCTCTG	SALK_068787
	GSP right	CAATGGCTGAATTACGGTGA	
	BP	LBB1.3 salk	

LBB1.3 salk	ATTTTGCCGATTTCGGAAC
JMLB1	GGCAATCAGCTGTTGCCCGTCTCACTGGTG

TABLE S3 - *Arabidopsis* plant lines used, with their origin and selection method

Plant line	Origin	SALK/ NASC code	selection marker	additional information
pWOX2::NLS:YFP	T. Laux		ppt	Breuninger et al. 2008
DR5::RFP	E. Benkova		hyg	Marhavý et al. 2011
arf7-1 arf19-1	NASC	N24629	PCR	Okushima et al. 2005
arf7-1 arf19-2	NASC	N24630	PCR	Okushima et al. 2005
tir1-1	NASC	N3798	PCR	Ruegger et al. 1997, 1998
afb1-3	NASC	SALK_070172C / N662878	PCR	
afb2-3	NASC	SALK_137151 / N637151	PCR	
afb3	NASC	SALK_016356C / N657515	PCR	
afb1-3 afb3-4	M. Estelle	SALK_070172 (afb1-3) SALK_068787 (afb3-4)	PCR	Dharmasiri et al. 2005, selected from segregating TirQ
tir1-1 afb3-4	M. Estelle	SALK_068787 (afb3-4)	PCR	Dharmasiri et al. 2005, selected from segregating TirQ
tir1-1 afb1-3	M. Estelle	SALK_070172 (afb1-3)	PCR	Dharmasiri et al. 2005, selected from segregating TirQ
arf5-1	NASC	SALK_023812/ N24605	PCR, *mp* phenotype	
arf6-1	NASC	N24606	PCR	
UAS::miR167a	J. Reed			Wu and Reed, unpublished
pRPS5a::GAL4	J. Reed / R. Offringa			Weijers et al. 2001
pARFxx::SV40x3GFP	D. Weijers		kan	Rademacher, E. PhD thesis (2009)
iaa14-1	NASC	N25214 / CS25214		
slr-1	H. Fukaki		LR phenotype	Fukaki et al. 2002
slr-1R1	H. Fukaki			Fukaki et al. 2002
pIAA14::GUS	H. Fukaki			Fukaki et al. 2002
pIAA14:mIAA14:GFP	H. Fukaki			Fukaki et al. 2002
pIAA14::IAA14 G79E (med)	J. Nemhauser		kan	T3, Guseman et al. 2015

TABLE S3 - *Arabidopsis* plant lines used, with their origin and selection method (continued)

Plant line	Origin	SALK/ NASC code	selection marker	additional information
pIAA14::IAA14 P81S (insensitive)	J. Nemhauser		kan	T3, Guseman et al. 2015
pIAA14::IAA14 G79E (med) DR5::Venus-N7	J. Nemhauser		kan x ppt	T3, Guseman et al. 2015
pIAA14::IAA14 P81S (insensitive) DR5::Venus-N7	J. Nemhauser		kan x ppt	T3, Guseman et al. 2015
pTIR1::cTIR1-GUS (tir1-1)	M. Estelle			Dharmasiri et al 2005, Parry et al. 2009
pAFB1::cAFB1-GUS (afb1-3)	M. Estelle			Dharmasiri et al 2005, Parry et al. 2009
pAFB2::cAFB2-GUS (afb2-3)	M. Estelle			Dharmasiri et al 2005, Parry et al. 2009
pAFB3::cAFB3-GUS (afb3-4)	M. Estelle			Dharmasiri et al 2005, Parry et al. 2009
iaa14-1	NASC	N25214 / CS25214		Overvoorde et al. 2005
slr-1	H. Fukaki		LR phenotype	Fukaki et al. 2002
slr-1R1	H. Fukaki			Fukaki et al. 2002
pIAA14::GUS	H. Fukaki			Fukaki et al. 2002
pIAA14:mIAA14:GFP	H. Fukaki			Fukaki et al. 2002
pIAA14::IAA14 G79E (med)	J. Nemhauser		kan	T3, Guseman et al. 2015
pIAA14::IAA14 P81S (insensitive)	J. Nemhauser		kan	T3, Guseman et al. 2015
pIAA14::IAA14 G79E (med) DR5::Venus-N7	J. Nemhauser		kan x ppt	T3, Guseman et al. 2015
pIAA14::IAA14 P81S (insensitive) DR5::Venus-N7	J. Nemhauser		kan x ppt	T3, Guseman et al. 2015
pTIR1::cTIR1-GUS (tir1-1)	M. Estelle			Dharmasiri et al 2005, Parry et al. 2009
pAFB1::cAFB1-GUS (afb1-3)	M. Estelle			Dharmasiri et al 2005, Parry et al. 2009
pAFB2::cAFB2-GUS (afb2-3)	M. Estelle			Dharmasiri et al 2005, Parry et al. 2009
pAFB3::cAFB3-GUS (afb3-4)	M. Estelle			Dharmasiri et al 2005, Parry et al. 2009

References

Adams-Cioaba, M.A., Li, Z., Tempel, W., Guo, Y., Bian, C., Li, Y., Lam, R., and Min, J. (2012). Crystal structures of the Tudor domains of human *PHF20* reveal novel structural variations on the Royal Family of proteins. FEBS Lett. **586**: 859–865.

Atta, R., Laurens, L., Boucheron-Dubuisson, E., Guivarc'h, A., Carnero, E., Giraudat-Pautot, V., Rech, P., and Chriqui, D. (2008). Pluripotency of *Arabidopsis* xylem pericycle underlies shoot regeneration from root and hypocotyl explants grown in vitro. Plant J. **57**: 626–644.

Boer, D.R., Freire-Rios, A., Van Den Berg, W.A.M., Saaki, T., Manfield, I.W., Kepinski, S., Lopez-Vidrieo, I., Franco-Zorrilla, J.M., De Vries, S.C., Solano, R., Weijers, D., and Coll, M. (2014). Structural basis for DNA binding specificity by the auxin-dependent *ARF* transcription factors. Cell **156**: 577–589.

Breuninger, H., Rikirsch, E., Hermann, M., Ueda, M., and Laux, T. (2008). Differential expression of WOX Genes mediates apical-basal axis formation in the *Arabidopsis* embryo. Dev. Cell **14**: 867–876.

Calderón Villalobos, L.I.A., Lee, S., De Oliveira, C., Ivetac, A., Brandt, W., Armitage, L., Sheard, L.B., Tan, X., Parry, G., Mao, H., Zheng, N, Napier, R., Kepinski, S., and Estelle, M. (2012). A combinatorial TIR1/AFB-Aux/IAA co-receptor system for differential sensing of auxin. Nat. Chem. Biol. **8**: 477–485.

Dharmasiri, N., Dharmasiri, S., and Estelle, M. (2005a). The F-box protein TIR1 is an auxin receptor. Nature **435**: 441–445.

Dharmasiri, N., Dharmasiri, S., Weijers, D., Lechner, E., Yamada, M., Hobbie, L., Ehrismann, J.S., Jürgens, G., and Estelle, M. (2005b). Plant development is regulated by a family of auxin receptor F box proteins. Dev. Cell **9**: 109–119.

DiDonato, R.J., Arbuckle, E., Buker, S., Sheets, J., Tobar, J., Totong, R., Grisafi, P., Fink, G.R., and Celenza, J.L. (2004). *Arabidopsis ALF4* encodes a nuclear-localized protein required for lateral root formation. Plant J. **37**: 340–353.

Dubrovsky, J.G., Napsucialy-Mendivil, S., Duclercq, J., Cheng, Y., Shishkova, S., Ivanchenko, M.G., Friml, J., Murphy, A.S., and Benková, E. (2011). Auxin minimum defines a developmental window for lateral root initiation. New Phytol. **191**: 970–983.

Fan, M., Xu, C., Xu, K., and Hu, Y. (2012). LATERAL ORGAN BOUNDARIES DOMAIN transcription factors direct callus formation in *Arabidopsis* regeneration. Cell Res. **22**: 1169–1180.

Fukaki, H., Nakao, Y., Okushima, Y., Theologis, A., and Tasaka, M. (2005). Tissue-specific expression of stabilized SOLITARY-ROOT/IAA14 alters lateral root development in *Arabidopsis.* Plant J. **44**: 382–395.

Fukaki, H., Tameda, S., Masuda, H., and Tasaka, M. (2002). Lateral root formation is blocked by a gain-of-function mutation in the *SOLITARY-ROOT/IAA14* gene of Arabidopsis. Plant J. **29**: 153–168.

Gaj, M.D. (2011). Somatic embryogenesis and plant regeneration in the culture of *Arabidopsis thaliana* (L.) Heynh. immature zygotic embryos. Methods **710**: 257–265.

Giraudat, J. (2003). Practical course on genetic and molecular analysis of *Arabidopsis*. In EMBO course, J. Giraudat, ed (EMBO), pp. 1–21.

Goh, T., Kasahara, H., Mimura, T., Kamiya, Y., and Fukaki, H. (2012). Multiple *AUX/IAA-ARF* modules regulate lateral root formation: the role of *Arabidopsis SHY2/IAA3*-mediated auxin signalling. Philos. Trans. R. Soc. Lond. B. Biol. Sci. **367**: 1461–1468.

Guilfoyle, T.J. (2015). The *PB1* domain in auxin response factor and Aux/IAA proteins: a versatile protein interaction module in the auxin response. Plant Cell **27**: 33–43.

Guilfoyle, T.J. and Hagen, G. (2007). Auxin response factors. Curr. Opin. Plant Biol. **10**: 453–460.

Guseman, J.M., Hellmuth, A., Lanctot, A., Feldman, T.P., Moss, B.L., Klavins, E., Calderon Villalobos, L.I.A., and Nemhauser, J.L. (2015). Auxin-induced degradation dynamics set the pace for lateral root development. Development **142**: 905–909.

Gutierrez, L., Bussell, J.D., Pacurar, D.I., Schwambach, J., Pacurar, M., and Bellini, C. (2009). Phenotypic plasticity of adventitious rooting in *Arabidopsis* is controlled by complex regulation of *AUXIN RESPONSE FACTOR* transcripts and microRNA abundance. Plant Cell **21**: 3119–3132.

Gutierrez, L., Mongelard, G., Floková, K., Pacurar, D.I., Novák, O., Staswick, P., Kowalczyk, M., Pacurar, M., Demailly, H., Geiss, G., and Bellini, C. (2012). Auxin controls *Arabidopsis* adventitious root initiation by regulating jasmonic acid homeostasis. Plant Cell **24**: 2515–2527.

Hardtke, C.S. and Berleth, T. (1998). The *Arabidopsis* gene *MONOPTEROS* encodes a transcription factor mediating embryo axis formation and vascular development. EMBO J. **17**: 1405–1411.

Hayashi, K.-I., Tan, X., Zheng, N., Hatate, T., Kimura, Y., Kepinski, S., and Nozaki, H. (2008). Small-molecule agonists and antagonists of F-box protein-substrate interactions in auxin perception and signaling. Proc. Natl. Acad. Sci. USA **105**: 5632–5637.

Hayashi, K., Neve, J., Hirose, M., Kuboki, A., Shimada, Y., Kepinski, S., and Nozaki, H. (2012). Rational design of an auxin antagonist of the SCF(TIR1) auxin receptor complex. ACS Chem. Biol. **7**: 590–598.

Holmes, D., Moody, P., and Dine, D. (2011). Research methods for biosciences 2nd ed. Oxford University Press.

Ikeuchi, M., Sugimoto, K., and Iwase, A. (2013). Plant callus: mechanisms of induction and repression. Plant Cell **25**: 3159–3173.

Korasick, D. A, Westfall, C.S., Lee, S.G., Nanao, M.H., Dumas, R., Hagen, G., Guilfoyle, T.J., Jez, J.M., and Strader, L.C. (2014). Molecular basis for AUXIN RESPONSE FACTOR protein interaction and the control of auxin response repression. Proc. Natl. Acad. Sci. USA **111**: 5427–5432.

Krogan, N.T., Ckurshumova, W., Marcos, D., Caragea, A.E., and Berleth, T. (2012). Deletion of *MP/ARF5* domains III and IV reveals a requirement for *Aux/IAA* regulation in *Arabidopsis* leaf vascular patterning. New Phytol. **194**: 391–401.

Kurczyńska, E.U., Gaj, M.D., Ujczak, A., and Mazur, E. (2007). Histological analysis of direct somatic embryogenesis in *Arabidopsis thaliana* (L.) Heynh. Planta **226**: 619–628.

Lee, S., Sundaram, S., Armitage, L., Evans, J.P., Hawkes, T., Kepinski, S., Ferro, N., and Napier, R.M. (2014). Defining binding efficiency and specificity of auxins for SCF TIR1/AFB -Aux/IAA co-receptor complex formation. ACS Chem. Biol. **9**: 673–682.

Luo, Y. and Koop, H.U. (1997). Somatic embryogenesis in cultured immature zygotic embryos and leaf protoplasts of *Arabidopsis* thaliana ecotypes. Planta **202**: 387–396.

Malamy, J.E. and Benfey, P.N. (1997). Organization and cell differentiation in lateral roots of *Arabidopsis thaliana*. Development **124**: 33–44.

Maraschin, F.D.S., Memelink, J., and Offringa, R. (2009). Auxin-induced, SCF(TIR1)-mediated poly-ubiquitination marks AUX/IAA proteins for degradation. Plant J. **59**: 100–109.

Marhavý, P., Bielach, A., Abas, L., Abuzeineh, A., Duclercq, J., Tanaka, H., Pařezová, M., Petrášek, J., Friml, J., Kleine-Vehn, J., and Benková, E. (2011). Cytokinin modulates endocytic trafficking of PIN1 auxin efflux carrier to control plant organogenesis. Dev. Cell **21**: 796–804.

Nagpal, P., Ellis, C.M., Weber, H., Ploense, S.E., Barkawi, L.S., Guilfoyle, T.J., Hagen, G., Alonso, J.M., Cohen, J.D., Farmer, E.E., Ecker, J.R., and Reed, J.W. (2005). Auxin response factors

ARF6 and *ARF8* promote jasmonic acid production and flower maturation. Development **132**: 4107–4118.

Nowak, K., Wojcikowska, B., Szyrajew, K., and Gaj, M.D. (2012). Evaluation of different embryogenic systems for production of true somatic embryos in *Arabidopsis*. Biol. Plant. **56**: 401–408.

Okushima, Y., Overvoorde, P.J., Arima, K., Alonso, J.M., Chan, A., Chang, C., Ecker, J.R., Hughes, B., Lui, A., Nguyen, D., Onodera, C., Quach, H., Smith, A., Yu, G., and Theologis, A. (2005). Functional genomic analysis of the AUXIN RESPONSE FACTOR gene family members in *Arabidopsis thaliana*: unique and overlapping functions of *ARF7* and *ARF19*. Plant Cell **17**: 444–463.

Overvoorde, P.J., Okushima, Y., Alonso, J.M., Chan, A., Chang, C., Ecker, J.R., Hughes, B., Lui, A., Onodera, C., Quach, H., Smith, A., Yu, G., and Theologis, A. (2005). Functional genomic analysis of the *AUXIN/INDOLE-3-ACETIC ACID* gene family members in *Arabidopsis thaliana*. Plant Cell **17**: 3282–3300.

Pace, L. (2015). Beginning R: an introduction to statistical programming (Apress).

Parry, G., Calderon-Villalobos, L.I.A., Prigge, M., Peret, B., Dharmasiri, S., Itoh, H., Lechner, E., Gray, W.M., Bennett, M., and Estelle, M. (2009). Complex regulation of the *TIR1/AFB* family of auxin receptors. Proc. Natl. Acad. Sci. USA **106**: 22540–22545.

Piya, S., Shrestha, S.K., Binder, B., Stewart, C.N., and Hewezi, T. (2014). Protein-protein interaction and gene co-expression maps of ARFs and Aux/IAAs in *Arabidopsis.* Front. Plant Sci. **5**: 1–9.

Rademacher, E.H., Lokerse, A.S., Schlereth, A., Llavata-Peris, C., Bayer, M., Kients, M., Rios, A.F., Borst, J.W., Lukowitz, W., Jürgens, G., and Weijers, D. (2012). Different auxin response machineries control distinct cell fates in the early plant embryo. Dev. Cell **22**: 211–222.

Rademacher, E.H., Möller, B., Lokerse, A.S., Llavata-Peris, C.I., van den Berg, W., and Weijers, D. (2011). A cellular expression map of the *Arabidopsis AUXIN RESPONSE FACTOR* gene family. Plant J. **68**: 597–606.

Raghavan, V. (2004). Role of 2,4-dichlorophenoxyacetic acid (2,4-D) in somatic embryogenesis on cultured zygotic embryos of *Arabidopsis*: cell expansion, cell cycling, and morphogenesis during continuous exposure of embryos to 2,4-D. Am. J. Bot. **91**: 1743–56.

Robert, H.S., Grones, P., Stepanova, A.N., Robles, L.M., Lokerse, A.S., Alonso, J.M., Weijers, D., and Friml, J. (2013). Local auxin sources orient the apical-basal axis in *Arabidopsis* embryos. Curr. Biol. **23**: 2506–2512.

De Rybel, B., Vassileva, V., Parizot, B., Demeulenaere, M., Grunewald, W., Audenaert, D., Van Campenhout, J., Overvoorde, P., Jansen, L., Vanneste, S., Möller, B., Wilson, M., Holman, T., Van Isterdael, G., Brunoud, G., Vuylsteke, M., Vernoux, T., De Veylder, L., Inzé, D., Weijers, D., and Bennett, M.J. (2010). A novel Aux/IAA28 signaling cascade activates GATA23-dependent specification of lateral root founder cell identity. Curr. Biol. **20**: 1697–1706.

Scheres, B., Wolkenfelt, H., Willemsen, V., Terlouw, M., Lawson, E., Dean, C., and Weisbeek, P. (1994). Embryonic origin of the *Arabidopsis* primary root and root meristem initials. Development **2487**: 2475–2487.

Schlereth, A., Möller, B., Liu, W., Kientz, M., Flipse, J., Rademacher, E.H., Schmid, M., Jürgens, G., and Weijers, D. (2010). *MONOPTEROS* controls embryonic root initiation by regulating a mobile transcription factor. Nature **464**: 913–916.

De Smet, I., Lau S.,, Voß, U., Vanneste, S., Benjamins, R., Rademacher, E., Schlerethd, A., De Rybel, B., Vassileva, V., Grunewald, W., Naudts, M., Levesqueh, M.P., Ehrismann, J.S., Inzé, D., Luschnig, C., Benfey P.N., Weijers, D., Van Montagu, M.C.E., Bennett, M.J., Jürgens, G., and Beeckman, T., (2010). Bimodular auxin response controls organogenesis in *Arabidopsis*. Proc. Natl. Acad. Sci. USA **107**: 2705–2710.

Su, Y.H., Liu, Y.B., Zhou, C., Li, X.M., and Zhang, X.S. (2016). The microRNA167 controls somatic embryogenesis in *Arabidopsis* through regulating its target genes *ARF6* and *ARF8*. Plant Cell. Tissue Organ Cult. **124**: 405–417.

Su, Y.H. and Zhang, X.S. (2014). The hormonal control of regeneration in plants. Curr. Top. Dev. Biol. **108**: 35–69.

Sugimoto, K., Jiao, Y., and Meyerowitz, E.M. (2010). *Arabidopsis* regeneration from multiple tissues occurs via a root development pathway. Dev. Cell **18**: 463–471.

Swarup, K., Benková, E., Swarup, R., Casimiro, I., Péret, B., Yang, Y., Parry, G., Nielsen, E., De Smet, I., Vanneste, S., Levesque, M.P., Carrier, D., James, N., Calvo, V., Ljung, K., Kramer, E., Roberts, R., Graham, N., Marillonnet, S., Patel, K., Jones, J.D.G., Taylor, G., Schachtman, D.P., May, S., Sandberg, G., Benfey, P., Friml, J., Kerr, I., Beeckman, T., Laplaze, L., and Bennet, M.J. (2008). The auxin influx carrier LAX3 promotes lateral root emergence. Nat. Cell Biol. **10**: 946–954.

Tiwari, S.B., Hagen, G., and Guilfoyle, T.J. (2003). The roles of auxin response factor domains in auxin-responsive transcription. Plant Cell **15**: 533–543.

Ulmasov, T., Murfett, J., Hagen, G., and Guilfoyle, T.J. (1997). Aux/IAA proteins repress expression of reporter genes containing natural and highly active synthetic auxin response elements. Plant Cell **9**: 1963–71.

Wang, R. and Estelle, M. (2014). Diversity and specificity: auxin perception and signaling through the TIR1/AFB pathway. Curr. Opin. Plant Biol. **21C**: 51–58.

Weijers, D., Franke-van Dijk, M., Vencken, R.-J., Quint, A., Hooykaas, P. J.J., and Offringa, R. (2001). An *Arabidopsis* Minute-like phenotype caused by a semi-dominant mutation in a *RIBOSOMAL PROTEIN S5* gene. Development **128**: 4289–4299.

Weijers, D., Schlereth, A., Ehrismann, J.S., Schwank, G., Kientz, M., and Jürgens, G. (2006). Auxin triggers transient local signaling for cell specification in *Arabidopsis* embryogenesis. Dev. Cell **10**: 265–270.

Weijers, D. and Wagner, D. (2016). Transcriptional responses to the auxin hormone. Annu. Rev. Plant Biol. **67**: 539–574.

Wójcik, A.M. and Gaj, M.D. (2016). *miR393* contributes to the embryogenic transition induced in vitro in *Arabidopsis* via the modification of the tissue sensitivity to auxin treatment. Planta: 231–243.

Wright, R.C. and Nemhauser, J.L. (2015). New tangles in the auxin signaling web. F1000Prime Rep. **7**: 7-19.

Wu, M.-F., Tian, Q., and Reed, J.W. (2006). *Arabidopsis microRNA167* controls patterns of *ARF6* and *ARF8* expression, and regulates both female and male reproduction. Development **133**: 4211–4218.

Yoshida, S., Barbier de Reuille, P., Lane, B., Bassel, G.W., Prusinkiewicz, P., Smith, R.S., and Weijers, D. (2014). Genetic control of plant development by overriding a geometric division rule. Dev. Cell. 29: 75-87.